NAIC-ID(RS)T-0652-93

NATIONAL AIR INTELLIGENCE CENTER

A MULTI-WAVELENGTH DYE LASER SYSTEM

by

Tang Xingli, Shang-guan Cheng, et al.

HUMAN TRANSLATION

NAIC-ID(RS)T-0652-93 25 April 1995

MICROFICHE NR: 95C000239

A MULTI-WAVELENGTH DYE LASER SYSTEM

By: Tang Xingli, Shang-guan Cheng, et al.

English pages: 9

Source: Guangxue Xuebao, Vol. 12, Nr. 8, August 1992; pp. 684-687

Country of origin: China
Translated by: Leo Kanner Associates
F33657-88-D-2188
Requester: NAIC/TATD/Capt Meckler

GRAPHICS DISCLAIMER

All figures, graphics, tables, equations, etc. merged into this translation were extracted from the best quality copy available.

A MULTI-WAVELENGTH DYE LASER SYSTEM

Tang Xingli, Shang-guan Cheng, Lin Yingyi, Yu Kaiyi, Dou Airong, Wang Yiman, Sun Guohua, Jiang Sengli, Wang Wei, and Qian Yulan,
Shanghai Institute of Optics and Fine Mechanics, Chinese Academy of Sciences, Shanghai 201800.

Abstract

A four-wavelength dye laser system consisted of four dye lasers is developed. Its laser parameters and time characteristic after mixing four beams have been measured. The factors which have an effect on efficient dye laser power are discussed briefly. The total average output power of this system is 8.9 W.

Key words dye laser.

In many experiments on the interaction between the laser spectrum and the laser, on the one hand, and atomic vapor, on the other, oftentimes researchers study excitation and ionization of multi-color multi-photons, with the requirement of simultaneously focusing multi-wavelength laser beams in the interaction zone. Thus, it is required that multiple dye lasers operate simultaneously, and mix the various dye laser beams into a single beam. Recently, the authors developed a dye laser system composed of four dye lasers, pumped with a copper vapor laser. Fig. 1 is a block diagram of this laser system. The directivity

diameter of the light beam is OD30mm [1]. Passing a 1:3 hole shrinking lens set, the copper vapor laser was admitted into the dye laser. DL_1 and DL_2 were pumped with yellow-green light; DL_3 was pumped with pure yellow light; and DL_4 was pumped with pure green light. Based on experimental requirements for wavelength, these four dye lasers can select different dyes and solvents.

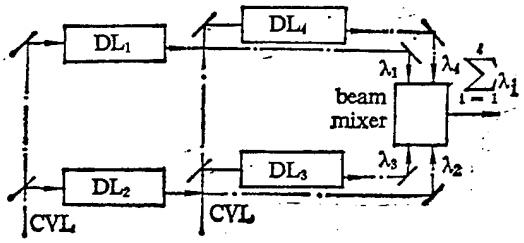

Fig. 1 Schemetic diagram of the dye laser system

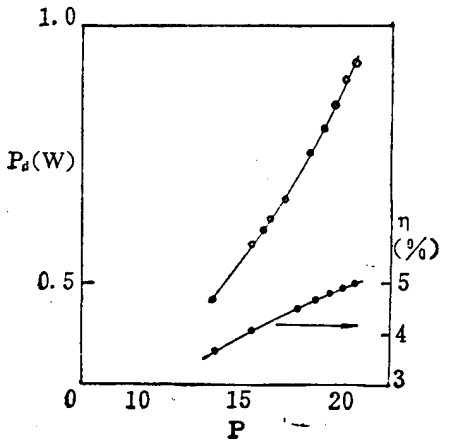

Fig. 2 Output power of dye laser as a function of pumping power (CVL) dye: Kiton red S, soluent: methanol

Each dye laser was an oscillation-amplification system of first-level oscillation and second-level amplification [2]. For the oscillators, a Littrow type grating cavity was used. As the wavelength selection element, the graduated grating employed 70 as the beam expander for the 600 lines per millimeter lens beam expander. The free spectrum range (of the standard device in the cavity) was $\nu_{FSR}=20\,GHz$; the finest degree was $F^{*}=16$, to

effectively narrow the spectral linewidth by compression.

When the laser dye operated with Kiton red S dye, the efficiency curve and the output power $P_d(W)$ was indicated as function of pumping power P, as shown in Fig. 2. At this time, the dye concentration (of the oscillation level) was $c_1=1.2\times10^{-3}$mol/L; the dye concentration (of the amplification-level) was $c_2=4.5\times10^{-4}$mol/L, with methyl alcohol as solvent. By measuring the dye laser linewidth $\Delta\lambda=0.001\,\mathrm{nm}$, the interference ring picture is shown in Fig. 3. The tuning curves of the range were between 588.0 and 631.0nm; the tuning curves of the output power $P_d(W)$, varying with wavelength lambda, are shown in Fig. 4. This is the measurement result of two situations, with and without placing a standard device in the cavity. From the curves in the figure, with approaching of the peak portion of the tuning curve when a standard device is placed in the cavity, the decrease in the dye laser output power was smaller. However, when the standard device was placed at the two flanks of the tuning curve, the reduction in laser power was relatively clear. Therefore, when selecting dyes we should let the operating wavelength be as close as possible to the peak portion of the dye tuning curve.

Since variation in dye temperature seriously affects the stability of the dye laser wavelength, temperature control systems are installed at the oscillation level of each dye laser set in order to control dye temperature. Thus, scanning of the

dye laser wavelength can be automatically controlled.

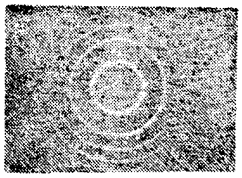

Fig. 3 Interference fringe of dye laser measuring etalon $d=10$ mm $\nu_{FSR}=10$ GHz

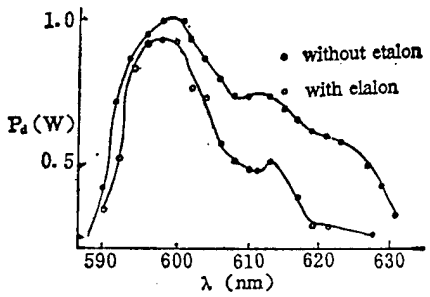

Fig. 4 Tuning of dye laser wavelength (dye solution: Kiton red S in methanol)

Dye laser beams of four different wavelengths were mixed into a single light beam. In other words, collinear and equal-diameter light beams are required in space, and synchronous in time. After beam mixing with the beam-mixing system of two dye laser beams, the complete coincidence is 91.8%. The efficiency of the beam-mixing system was approximately 85% [3]. The total power of the dye laser system was 8.9W. After beam mixing, the total power of the dye laser was 7.5W; the fractional power of each dye laser device was also measured. Table 1 lists the power data for a laser pumped with a copper vapor laser, and the corresponding efficiencies of dye lasers. For the dye laser system, its efficiency eta is the summation of various fractional powers of the wavelength dye lasers divided by the total pumping laser power. In other words,

$$\eta = \frac{P_d}{P} = \frac{\sum_{i=1}^{4} P_{di}}{\sum_{i=1}^{4} P_i} \qquad (1)$$

Calculating based on the above equation, eta=8.9%.

When the multi-wavelength dye laser system was used in multiple-step excitation and ionization experiments, since the absorption cross-sectional surfaces of different transitions were different, and sometimes the differences may be large, now we should base our procedures on the research objects to adjust the output power ratio of different wavelength dye lasers. enerally, for a transition with greater absorption cross-sectional areas the dye laser intensity used in excitation can be reduced. However, for a transition with a smaller absorption cross-sectional areas, the dye laser intensity used in excitation should be raised. For the excitation of multiple energy levels, appropriate intensity ratios should be selected for dye lasers with different wavelengths, then the final efficiency of interaction can be increased.

After mixing the four-wavelength dye laser beams, their time properties were measured. Table 2 lists the data of the measurement results.

The synchronizing situation of four-wavelength dye laser waveform was measured with the signal input type 4400 digital averager; the results are shown in Fig. 5.

Based on the results obtained, the time difference of the peak values for the $lambda_1$ and $lambda_2$ lasers was the largest;

$\tau_{14}=5.5\,ns$. Fig. 6 is a waveform overlapping diagram for a dye laser with four wavelengths. When examining the time coincidence of the pulse dye laser, calculations should be done with the two pulses that have the greatest time difference for the laser peak value.

Table 1 Output and efficiency of the dye laser system

	λ_1	λ_2	λ_3	λ_4	$\sum_{i=1}^{4}\lambda_i$
Output power of dye leser(W)	0.6	0.53	1.6	6.2	8.93
Pumping power (CVL) (W)	20.3	19.6	20.2	40.2	100.3
Efficiency(%)	3	3	8	15	8.9
Power of dye laser after beam mixing (W)	0.4	0.44	1.4	5.3	7.54

Table 2 Pulse duration and the time relation between pulses for dye laser

	λ_1	λ_2	λ_3	λ_4
Pulse duration of dye laser (ns)	28.4	28.5	26.2	28.1
Pulse duration of CVL (ns)	33	33	33	33
Relative time of the peak of dye laser pulse (ns)	32.0	33.7	35.2	37.5
Time between the peaks of two pulses (ns)	$\tau_{12}=1.7$	$\tau_{23}=1.5$	$\tau_{34}=2.3$	$\tau_{41}=5.5$
Repetition rate (kHz)	6			

Now, we examine the synchronizing property of two pulse waveforms. Assume that the two pulse waveforms are basically symmetrical: the pulse widths are, respectively, τ_a and τ_b . If $\tau_a>\tau_b$, the time difference of the peak values for the two pulses is τ_{ab}, then the time coincidence of two pulses is roughly

$$\eta_s=\begin{cases}1, & \tau_{ab}<(\tau_a-\tau_b)/2\\ \dfrac{\tau_b-[\tau_{ab}-(\tau_a-\tau_b)/2]}{\tau_b}, & \tau_{ab}\geqslant(\tau_a-\tau_b)/2\end{cases} \tag{2}$$

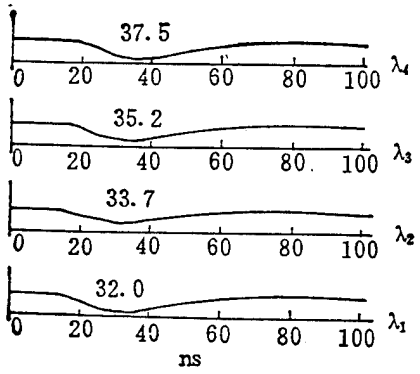

Fig. 5 Time behaviour of four-dye laser pulses

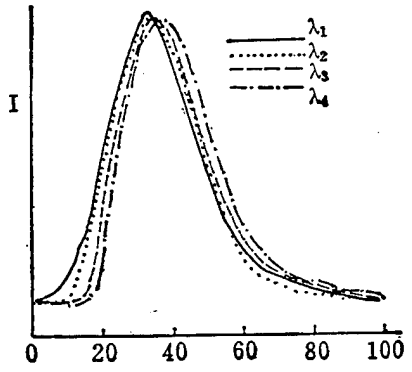

Fig. 6 Pulse overlap of four-dye laser

When we insert the time-property data of the lambda$_1$ and lambda$_4$ laser into Eq. (2), we obtain $\eta_s=81\%$, the time coincidence of the different wavelength dye lasers can be improved by optical path compensation. In the beam-mixing process, the optical path of various wavelengths was cautiously adjusted so that the time coincidence after beam mixing was the highest. Now, the time noncoincidence comes mainly, possibly, from discharge instability of the copper vapor laser. On the other hand, the widths of several pulses cannot differ too widely. If the difference is too large, the multistep excitation will be affected. This effect is closely related to the energy level lifetime of the excited material.

Before arriving at the interaction zone, the effective power

of the laser beam is the value obtained by multiplying the total output power P_d of the dye laser with the efficiency of various sectors such as beam mixing and synchronizing. That is,

$$P_e = P_d \eta_{c1} \eta_{c2} \eta_s = P \eta_d \eta_{c1} \eta_{c2} \eta_s. \quad (3)$$

In the equation, η_{c1} is the spatial coincidence of beam mixing; η_{c2} is the power efficiency of beam mixing; and η_d is the dye laser efficiency. Upon inserting measurement data, we obtain the following: $P_c=0.63P_d$. In other words, before the dye laser arrives at the interaction zone, due to wear and noncoincidence (among other factors), the effective power of the dye laser is about 63% of the total dye laser output power.

After the dye laser arrives at the interaction zone, due to the effect of other factors such as frequency drift, the interaction effect is weakened. This effect is related to the energy level width of the interacting substances. Therefore, the wear in various sections should be reduced in order to fabricate an effective dye laser system, for higher efficiency in each sector.

The authors are grateful to Pan Wenjie of the Tianjin Institute of Physical Chemical Engineering for supplying the time-property data; the authors are also grateful to comrades Liang Paihui et al for their assistance.

The first draft of the article was received on September 9, 1991. The final revised draft was received for publication on December 12, 1991.

REFERENCES

1. Liang Baogen, Fang Wuji, Zhang Fuyuan, et al, "20-W discharge heating type copper vapor laser," Zhongguo Jiguang [Lasers in China] 13/6, 334-347 (1986).

2. Shang-guan Cheng, Tang Xingli, Lin Yingyi, et al, "Dye laser pumped with 6.7W CVL," Zhongguo Jiguang 19/7, 481-485.

3. Xu Yuguang, Yu Leyue, Lu Bo et al, "Synthesizing and transport of multibeam laser," Zhongguo Jiguang 18/2, 98 (1991).

DISTRIBUTION LIST

DISTRIBUTION DIRECT TO RECIPIENT

ORGANIZATION	MICROFICHE
B085 DIA/RTS-2FI	1
C509 BALLOC509 BALLISTIC RES LAB	1
C510 R&T LABS/AVEADCOM	1
C513 ARRADCOM	1
C535 AVRADCOM/TSARCOM	1
C539 TRASANA	1
Q592 FSTC	4
Q619 MSIC REDSTONE	1
Q008 NTIC	1
Q043 AFMIC-IS	1
E051 HQ USAF/INET	1
E404 AEDC/DOF	1
E408 AFWL	1
E410 AFDTC/IN	1
E429 SD/IND	1
P005 DOE/ISA/DDI	1
P050 CIA/OCR/ADD/SD	2
1051 AFIT/LDE	1
P090 NSA/CDB	1
2206 FSL	1

Microfiche Nbr: FTD95C000239
NAIC-ID(RS)T-652-93